Radiation attenuation by lead and nonlead materials used in radiation shielding garments

J. P. McCaffrey,[a] H. Shen, B. Downton, and E. Mainegra-Hing
Ionizing Radiation Standards, National Research Council of Canada, Ottawa, Ontario K1A 0R6 Canada

(Received 7 July 2006; revised 30 October 2006; accepted for publication 28 November 2006; published 18 January 2007)

The attenuating properties of several types of lead (Pb)-based and non-Pb radiation shielding materials were studied and a correlation was made of radiation attenuation, materials properties, calculated spectra and ambient dose equivalent. Utilizing the well-characterized x-ray and gamma ray beams at the National Research Council of Canada, air kerma measurements were used to compare a variety of commercial and pre-commercial radiation shielding materials over mean energy ranges from 39 to 205 keV. The EGSnrc Monte Carlo user code `cavity.cpp` was extended to provide computed spectra for a variety of elements that have been used as a replacement for Pb in radiation shielding garments. Computed air kerma values were compared with experimental values and with the SRS-30 catalogue of diagnostic spectra available through the Institute of Physics and Engineering in Medicine Report 78. In addition to garment materials, measurements also included pure Pb sheets, allowing direct comparisons to the common industry standards of 0.25 and 0.5 mm "lead equivalent." The parameter "lead equivalent" is misleading, since photon attenuation properties for all materials (including Pb) vary significantly over the energy spectrum, with the largest variations occurring in the diagnostic imaging range. Furthermore, air kerma measurements are typically made to determine attenuation properties without reference to the measures of biological damage such as ambient dose equivalent, which also vary significantly with air kerma over the diagnostic imaging energy range. A single material or combination cannot provide optimum shielding for all energy ranges. However, appropriate choice of materials for a particular energy range can offer significantly improved shielding per unit mass over traditional Pb-based materials. [DOI: 10.1118/1.2426404]

I. INTRODUCTION

Radiation shielding garments are commonly used to protect medical patients and workers from exposure to direct and secondary radiation during diagnostic imaging in hospitals, clinics and dental offices. Similar materials are employed for other applications such as scanner curtains used to protect personnel working in the vicinity of airport scanners or similar devices. In most of these environments, typical peak x-ray energies range from 60 to 120 kVp, corresponding to mean energies of approximately 35–60 keV. The photoelectric effect overwhelmingly dominates energy transfer and absorption in this energy range, so only this mechanism is discussed in this study. The effectiveness of radiation shielding varies significantly with the photoelectric attenuation coefficients of the constituent materials, the thickness of the garments, and the energy spectrum of the radiation.

Historically, radiation shielding aprons and coverings have been manufactured from lead (Pb) powder-loaded polymer or elastomer sheets. Typical garment lifetime for these materials is approximately 10 years, although abuse can drastically shorten this period. Aging, damage, embrittlement, as well as cracking (particularly of garments incorporating natural rubber) results in drastically reduced lifetimes. Early studies of non-Pb materials were prompted by the desire to reduce the weight of protective garments and the possibility of improved shielding performance.[1]. The challenge has been to find processes that incorporate metal powders into polymer sheets with sufficient metal content for effective attenuation, but robust enough to avoid tearing, cracking and other forms of deterioration. Several more recent studies using clinical beams have examined different aspects of the attenuation properties of some commercial radiation aprons.[2–6] For example, the study by Christodoulou *et al.*[5] combines observations of inconsistencies in shielding performance with recommendations to improve standardized methods for acceptance testing.

Pb powder-loaded sheets are currently considered toxic materials, so disposal issues provide further motivation for the development of replacement garments containing non-Pb or Pb-combination materials to minimize Pb content. A typical Pb-based radiation shielding garment may contain approximately 0.5 m^2 of shielding material with a thickness of ~1.5 mm, with a mass of about 4.5 kg. This would provide the same protection as a garment composed of 0.5 mm pure Pb, which for the same area of material would have a mass of approximately 2.6 kg. The cover plus the rubber or polymer imbedding material account for the difference in mass. Non-Pb protective materials can lower the total mass of a similar sized garment, providing a decrease in the mass of the garment while providing equivalent or better protection. This current study includes attenuation measurements and comparisons of Pb sheets to actual Pb-based and non-Pb protective materials currently in use or under development for the radiation shielding market.

TABLE I. Elements incorporated into some commercial radiation-shielding garment materials.

ELEMENT	ATOMIC NO.	Density (g/cm^3)	K absorption edge (keV)
Cadmium (Cd)	48	8.65	26.7
Indium (In)	49	7.31	27.9
Tin (Sn)	50	7.30	29.2
Antimony (Sb)	51	6.69	30.5
Cesium (Cs)	55	1.87	36.0
Barium (Ba)	56	3.5	37.4
Cerium (Ce)	58	6.66	40.4
Gadolinium (Gd)	64	7.90	50.2
Tungsten (W)	74	19.3	69.5
Lead (Pb)	82	11.36	88.0
Bismuth (Bi)	83	9.75	90.5

Commercial radiation shielding garments may include some of the elemental powders shown in Table I, imbedded in natural rubber or various polymers. For the purposes of shielding, the energy of the *K* absorption edge is an important parameter in the diagnostic imaging range, as individual elements strongly absorb energy at levels immediately above their respective edges. To aid in visualizing the magnitude and values of this parameter, Fig. 1 displays the photon attenuation coefficients for elements with atomic numbers from 37 to 88, and their corresponding *K* absorption edges from 10 to 100 keV.[7] The atomic numbers (Z) are included on the right side of the graph, and the energy of the absorption edges in keV is given across the front of the graph. The position of the absorption edges for Pb (Z=82) at 88 keV and for Sn (Z=50) at 29 keV are highlighted in the figure. The magnitude of the photon attenuation coefficients abruptly rises at each *K* absorption edge, then gradually decreases above the edge. The resulting spectrum for these filter materials will show a rise in fluence before the absorption edge followed by a sharp drop at the edge, illustrated in the modeling section below. All elements become less effective at attenuating higher energy photons as the photoelectric effect becomes less relevant, requiring thicker layers for significant attenuation.

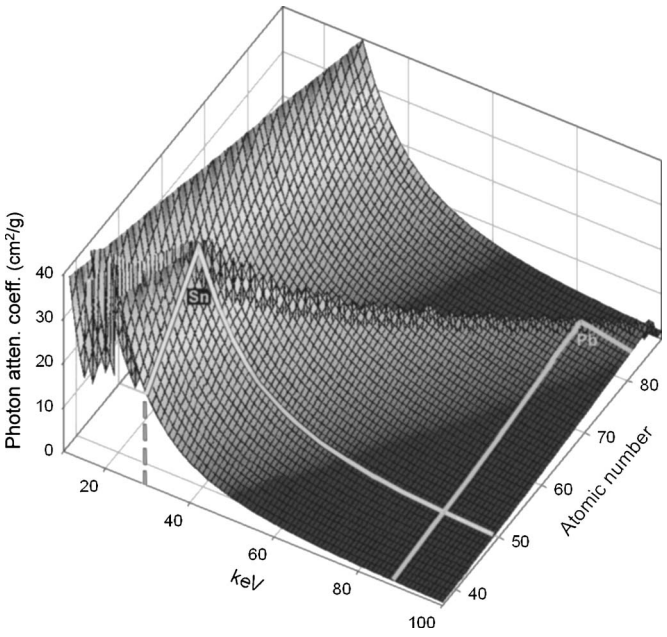

FIG. 1. Photon attenuation coefficients for elements with atomic numbers from 37 to 88, and their corresponding *K* absorption edges. The positions of the Pb and Sn *K* absorption edges are illustrated.

The purpose of this study is to correlate radiation attenuation, materials characterization, calculated spectra and ambient dose equivalent, over energy ranges from diagnostic imaging (60–120 kVp) up to therapy level energies (highly filtered 250 kVp), spanning mean energies from 39 to 205 keV. The highly characterized x-ray beams at the laboratories of the Ionizing Radiation Standards group of the National Research Council of Canada (NRC-the Canadian Primary Standards laboratory) were used in this study. Samples of radiation shielding materials were requested from several manufacturers, and this study examines the materials volunteered.

II. MATERIALS AND METHODS

Seven commercial and pre-commercial materials were investigated in this study: pure Pb, two Pb-based materials, one Pb–Sn material, and three non-Pb materials. The Pb-containing materials were checked for the presence of radioactivity, and no contributory signal above background radiation was detected. All materials were provided as thin sheets ranging in thickness from 0.25 to 2.0 mm. For all but one of these materials, the thin sheets were cut into squares approximately 15 cm × 15 cm. For the Sn–Ba material, only smaller pieces were available so these were mounted in holes cut in 15 cm × 15 cm Mylar support sheets. The dimensions of all of the individual sheets and pieces were carefully measured and weighed. W–rubber was counted as a single material, even though three different densities of W–rubber were supplied, as was Pb–rubber, where three different materials with two different densities were supplied. To facilitate intercomparisons of all seven materials, all were converted to thicknesses measured in g/cm^2 (density multiplied by thickness). This allowed direct comparisons of attenuation capabilities

TABLE II. The seven radiation shielding materials investigated in this study.

NAME	COMPOSITION	DENSITY (g/cm^3)
Pb	Pb	11.36
Pb–rubber	Pb–rubber	3.70, 4.10
Reg. lead	Pb–PVC vinyl	4.81
Hx–lead	Proprietary, Pb, PVC vinyl	4.45
W–rubber	W–rubber	4.15, 5.65, 7.51
Green Lite	Proprietary, PVC vinyl	3.68
Sn–Ba	Sn–Ba polymer	4.94

regardless of the density or composition of an individual thin sheet. The composition and density of the materials are given in Table II.

Variations in density for similar materials (Pb–rubber and Reg. Lead, for example) arise from differences in the relative percentage of metal incorporated, and to variations in the imbedding material. To measure the attenuation of increasing total thicknesses for each of the materials, stacks of thin sheets of all materials were used. In this study, only the basic attenuating materials, exclusive of the apron covering, were investigated.

A Lucite frame was constructed to support the stacks of thin sheets. The frame was mounted in a position typically used for radiation absorbers used in half value layer (HVL) measurements for x-ray qualities, approximately 5 cm downstream of the limiting aperture, in a narrow beam geometry. The free air chamber was positioned at the reference 1.0 m position for all radiation qualities, with a field size of 9 cm diameter. The choice of "good geometry" was determined by our choice of detector—a Primary Standards quality free air chamber. The free air chamber allowed us to very accurately determine the sometimes subtle differences in air kerma attenuation between materials in an identical geometry, but imposed limitations in addressing contributions from backscatter or off-axis K x rays. The entrant aperture for the free air chamber has a diameter of 10.01 mm, and the air volume from which charge is collected is a 10 cm column centered 39 cm farther downstream inside the free air chamber. As a result, off-axis photons, even generated very close to the entrant aperture, will not contribute to the collected charge.

Attenuation testing was performed for the materials with x-ray beams of six different energies (Table III). The six x-ray qualities were generated with a Comet MXR-320 x-ray tube. The NRC medium energy exposure standard (MEES) Primary Standard free-air chamber was used to determine the absolute measure of air kerma free in air. As well, the MEES was used to determine the relative attenuation of a variety of thicknesses of attenuating materials in the filter position. All charge readings from the MEES were normalized against a monitor chamber reading, which is routinely used to monitor the beam fluence rate. For attenuation comparisons, the ratios of the normalized x-ray qualities with additional attenuation (garment material) to the normalized basic x-ray qualities were used.

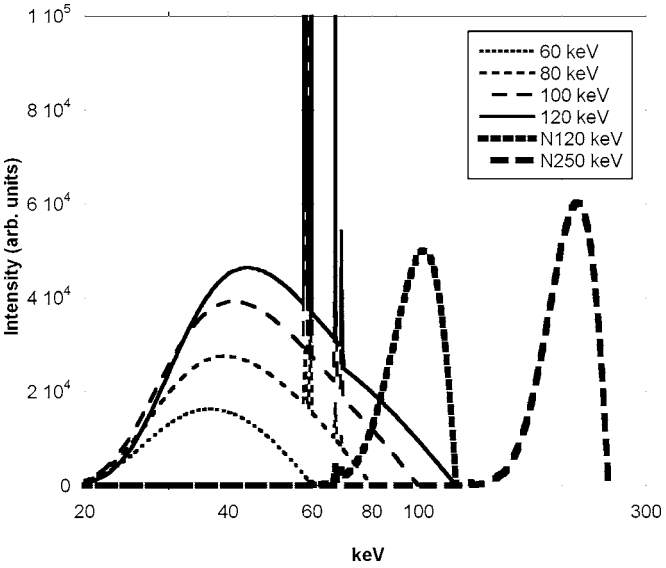

FIG. 2. Spectra of the six radiation qualities used in this study.

The first four x-ray qualities in Table III are representative of the range used clinically for diagnostic x-ray imaging: 60, 80, 100 and 120 kVp, with HVLs of ~3, 4, 5 and 6 mm Al, respectively. Two higher energy, radiation therapy x-ray qualities were also used: N120 and N250 kVp. Two of the diagnostic x-ray qualities, 80 and 120 kVp, were chosen to be similar to two qualities listed in the CEI 1331-1 International Standard, "Protective devices against diagnostic medical x radiation";[8] the 80 kVp quality (half value layer (HVL 4.3 mm Al) and 100 kVp quality (HVL 6.2 mm Al). The spectral shape of the six qualities is shown in Fig. 2. Note that the x axis is a log scale and the peak amplitudes are arbitrary, intended only to identify the relative positions and shapes of the spectra.

III. RESULTS

An initial series of measurements were made with nominally 0.25-mm-thick pure Pb sheets, stacked to provide 0.25,

TABLE III. The six radiation qualities used in this study. The "N" signifies a narrow spectrum series quality, i.e., high filtration.

kVp/ radio-nuclide	60	80	100	120	N120	N250
Mean keV	38.9	46.3	52.6	58.7	100	205
Filtration (mm)	5.15 Al	5.15 Al	5.15 Al	5.91 Al	5.0 Cu 1.0 Sn	2.5 Sn 2.5 Pb
HVL (mm)	2.96 Al	3.87 Al	4.79 Al	6.04 Al	1.72 Cu	5.2 Cu

TABLE IV. Effective transmission (%) of the six radiation qualities used in this study by different thicknesses of pure Pb.

	60 kVp	80 kVp	100 kVp	120 kVp	N120 kVp	N250 kVp
0.25 mm Pb	4.28%	11.95	16.73	20.16	30.11	77.52
0.5 mm Pb	0.42	2.55	4.96	6.31	10.05	60.50
1.0 mm Pb	0.01	0.27	0.86	1.09	1.63	37.13
2.0 mm Pb	0.00	0.01	0.05	0.06	0.16	14.20

0.5, 1.0, and 2.0 mm transmission values for each of the beam qualities (Table IV). These values of the air kerma transmission were used for comparison with the garment materials studied, since common figures of merit for specifying the attenuation capabilities of radiation shielding garments are "0.25 mm Pb equivalent," "0.5 mm Pb equivalent," etc. A particular Pb thickness corresponds to significantly different levels of transmission depending on the x-ray or gamma ray energy. Notice that for the four x-ray qualities representative of the range used for diagnostic x-ray imaging (60, 80, 100 and 120 kVp), 0.25 mm Pb equivalent covers a variation in air kerma transmission from approximately 4 to 20%.

The remaining six materials from Table II were measured in the same manner as for Pb. An example of the results for the 80 kVp beam quality is shown in Fig. 3. The percent transmission is given on the y axis, and the thickness of the material in g/cm^2 is given on the x axis. To illustrate a manner of extracting information from this graph, note the density of pure Pb from Table II, 11.36 g/cm^3. Multiplying 11.36 g/cm^3 by a thickness of 0.5 mm gives 0.568 g/cm^2. On the curve for pure Pb in Fig. 3 (large shaded circles), the thickness of 0.568 g/cm^2 on the x axis corresponds to a transmission level of 2.55% on the y axis. For clarity, this 2.55% transmission level is marked as a thick horizontal line across the graph, indicated by the arrow on the left (see also Table IV). The thickness for any of the other materials which is required to provide 0.5 mm Pb equivalency (2.55% transmission) can then be easily determined by

$$T_{Z(0.5)} = \frac{t_z}{\rho}.$$

$T_{Z(0.5)}$: thickness of material Z required to provide 0.5 mm Pb equivalency
t_z: thickness in g/cm^2 where the curve for material Z crosses the 0.5 mm Pb equivalency line, as taken from Fig. 3
ρ: density of material taken from Table II

For example, the corresponding thickness where the 80 kV Gr. Lite curve crosses the 2.55% line is 0.53 g/cm^2. Dividing this thickness (0.53 g/cm^2) by the density (3.68 g/cm^3, from Table II) gives a value of 1.44 mm; 1.44 mm of Gr. Lite is required to provide 0.5mm Pb equivalency at this 80 keV x-ray quality. Similarly for the W–rubber material, dividing the thickness indicated by where the 80 kV W-rubber curve crosses the 2.55% line (0.83 g/cm^2) by the density of material desired (4.15, 5.65, or 7.51 g/cm^3; Table II) gives the thickness of W–rubber required to attain 0.5 mm Pb equivalency: 2.00, 1.47, or 1.11 mm, respectively, for the three densities of W–rubber supplied. As a final example, for Reg. Lead, the 2.55% transmission level is found at a thickness of 0.67 g/cm^2, which corresponds to a required thickness of 1.39 mm.The relative mass for these aprons would therefore be: pure Pb=1.00, Gr.Lite=0.93, W–rubber=1.46, and Reg. Lead=1.17. This illustration supports manufacturers' claims that some nonlead aprons can have significantly less mass than traditional lead aprons.

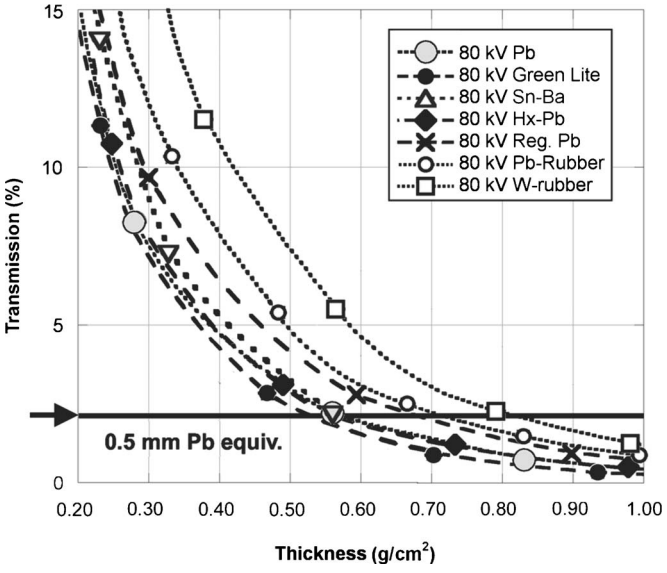

FIG. 3. Transmission vs thickness for the seven materials in this study at the 80 kVp x-ray quality.

The 0.25, 0.5, and 1.0 mm Pb equivalencies for the seven materials and six radiation qualities studied were determined as explained for Fig. 3 above, and are shown graphically in Figs. 4(a)–4(c). In these figures, the smaller a y value, the lower the mass required to provide the "Pb equivalent" appropriate for that plot. For reference, the horizontal dashed lines correspond to thicknesses of 0.25, 0.5, and 1.0 mm pure Pb (Figs. 4(a)–4(c), respectively). The Hx–Pb, Green Lite and Sn–Ba curves reach below the dotted horizontal lines in many cases, indicating that garments made of these materials require less mass than pure Pb for equivalent attenuation at the diagnostic imaging radiation qualities. Since pure Pb is not used as a radiation shielding garment, a more useful comparison is to the traditional Pb-containing materials (Reg. Pb and Pb–rubber), where these three non-Pb and Pb-combination materials show significant reductions in mass relative to Pb-containing materials, for equivalent attenuation of the three lower x-ray qualities. The W–rubber is not as effective for the 60 or 80 kVp x-ray qualities because of the W emission peaks near 60 and 70 keV (discussed below). However, at the four higher energies (and above), W performs nearly as well as the Pb–rubber and Reg. Pb garments, making the W–rubber a good choice as a non-Pb attenuator of higher energy x rays as well as gamma rays.

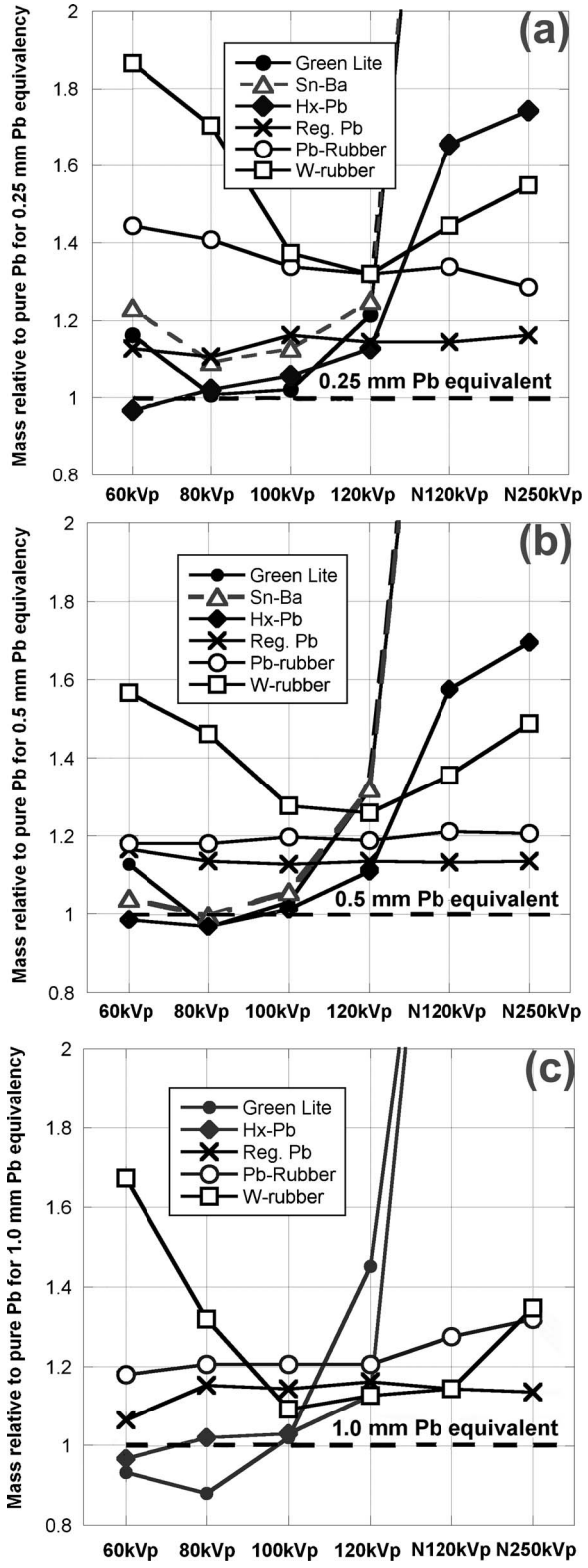

FIG. 4. Mass relative to pure Pb for (a) 0.25 mm, (b) 0.5 mm, and (c) 1.0 mm Pb equivalencies at six radiation qualities.

The Green Lite and Sn−Ba values rise above the plot in Figs. 4(a)–4(c) for the N120 and N250 keV qualities (values are approximately 3), indicating that these two non-Pb materials are not as effective for these x-ray qualities. Due to lack of sufficient material, Sn−Ba results are not provided for the higher energies in Fig. 4(b) or for any energies in Fig. 4(c). All materials studied varied in their attenuation response for all of the measured energies as well as for each thickness of Pb equivalent.

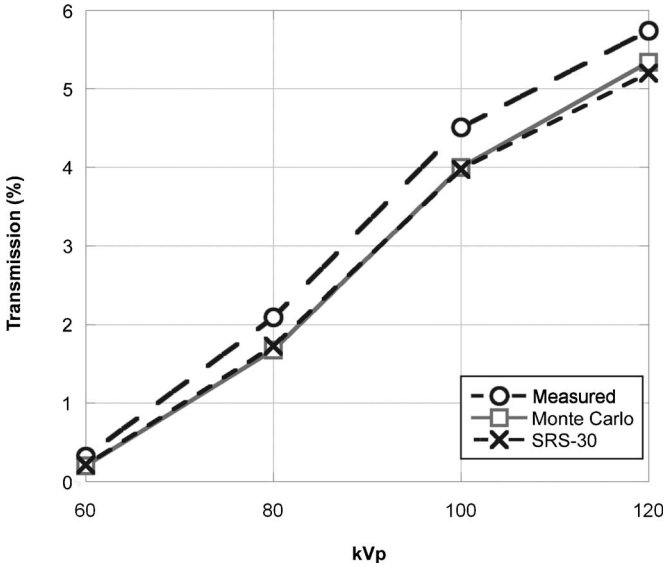

FIG. 5. Transmission of four x-ray qualities (*x*-axis) by 0.5 mm Pb: comparison of experimental, EGSnrc Monte Carlo calculations and IPEM report 78 values of attenuation.

For radiation protection garments, claims of 0.25 mm Pb equivalent, 0.5 mm Pb equivalent, etc., are ambiguous unless the radiation qualities are specified. A more meaningful figure of merit would include the degree of attenuation at a specific x-ray quality. For a Standards Laboratory, for example, a standard reference condition such as 2.6% transmission at 80 kVp, HVL 4 mm Al would be a useful reference condition. This reference condition is equivalent to 0.5 mm Pb at an x-ray quality suitable for encompassing most diagnostic imaging applications, and includes attenuation of the tungsten emission peaks.

IV. MODELING

The EGSnrc[9,10] user code `cavity.cpp`[11,12] was extended to provide calculated spectra for attenuation of the x-ray qualities by the elements in Table I used as Pb replacements in radiation shielding garments. To evaluate the accuracy of the code, Fig. 5 compares the transmission measurements of the 0.5 mm sheets of pure Pb at the four diagnostic x-ray qualities with transmission calculations using the EGSnrc code as well as with the Catalogue of Spectral Data for Diagnostic X rays (SRS-30), available through the Institute of Physics and Engineering in Medicine Report 78.[13] For the measured x-ray qualities, the B value (the total correction factor for a particular x-ray quality as measured by a particular free air chamber) was not accurately known for the beams containing the additional 0.5 mm Pb attenuation. However, the variation of B with effective energy was well known, so a small calculated correction factor was included in the measured values to correct for the change in hardness of the

beam quality due to the addition of the Pb. The air kerma measurements were performed with a Primary Standards free air chamber and have a combined uncertainty of 0.54% (coverage factor of $k=2$ and confidence level of 95%).[14] As most of the measured values used here are relative measurements, the uncertainty is, in fact, much lower. The measurements were taken at 100 cm source to detector distance.

The EGSnrc user code `cavity.cpp` generated comparison spectra in close agreement with experiment. The largest source of uncertainties in the EGSnrc spectra is contributed by the uncertainties in the XCOM[15] cross sections. These are estimated to range from 5 to 10%. The EGSnrc spectra and response were calculated at 100 cm source to detector distance.

The SRS-30 comparison spectra are based on a theoretical method developed by Birch and Marshall[16] which generates fitted results in close agreement with experimental spectra. These data depend on the unfolding of measured x-ray spectra as well as knowledge of the response function of the detectors. These comparison spectra were based on a source to detector distance of 75 cm. An additional available calculation, the SRS-30 HVL values, varied from the NRC measured values by 0.5–1.2% for 60–120 kVp spectra.

The positions of the K absorption edges are the most significant factors in choosing component materials for effective radiation shielding garments at diagnostic imaging energies. EGSnrc calculations of the 80 kVp fluence spectra produced by adding thin attenuating layers (filters) of six of the materials from Table I are shown in Fig. 6(a) (every tenth data point is shown, plus additional points for the W $K\alpha$ peaks). All spectra were calculated using the same filter mass for all materials (0.568 g/cm^2; equivalent to 0.5 mm thickness of Pb), but the physical thickness of the various filter materials varies. For example, the density of Ba is about 3.25 times lower than Pb, so Ba sheets 3.25 times thicker than the sheets of pure Pb must be used.

The similar K edge energy and higher atomic number of Bi relative to Pb shown in Fig. 6(a) allows a slight improvement over Pb (lower fluence, hence lower air kerma). However, of these five non-Pb elements shown here, the position of the Ba K absorption edge (37.4 keV) results in superior overall attenuation of this energy spectrum compared to Pb. The Ba is less effective at attenuating the radiation spectrum at energies below its K absorption edge of 37.4 keV, but improves significantly above that edge. For the 80 kVp quality, a Ba filter reduces the total air kerma by a factor of 2.06 over a Pb filter with equivalent mass (Fig. 7, discussed below). A similar example for the 60 kVp spectra is shown in Fig. 6(b), where the absence of the W $K\alpha$ peaks simplifies the fluence spectra considerably.

One quantity of interest in radiation protection is ambient dose equivalent $H^*(10)$, which is a measure of the biological damage at 10 mm depth incurred by tissue exposed to radiation.[17] The unit of measure is the J kg^{-1}, which has been given the special name of sievert (Sv). Ambient dose equivalent $H^*(10)$ at a point in a radiation field is the dose equivalent that would be produced by the corresponding expanded and aligned field in the International Commission on Radiation Units and Measurements sphere at a depth of 10 mm.[18] A practical advantage of this quantity in characterizing radiation shielding garments is that it can be calculated by multiplying the result of a simple air kerma measurement (in units of Gy) by a conversion coefficient $H_k^*(10)$.[17] In this study, $H^*(10)$ provides a sense of the effectiveness of the different materials used for radiation shielding.

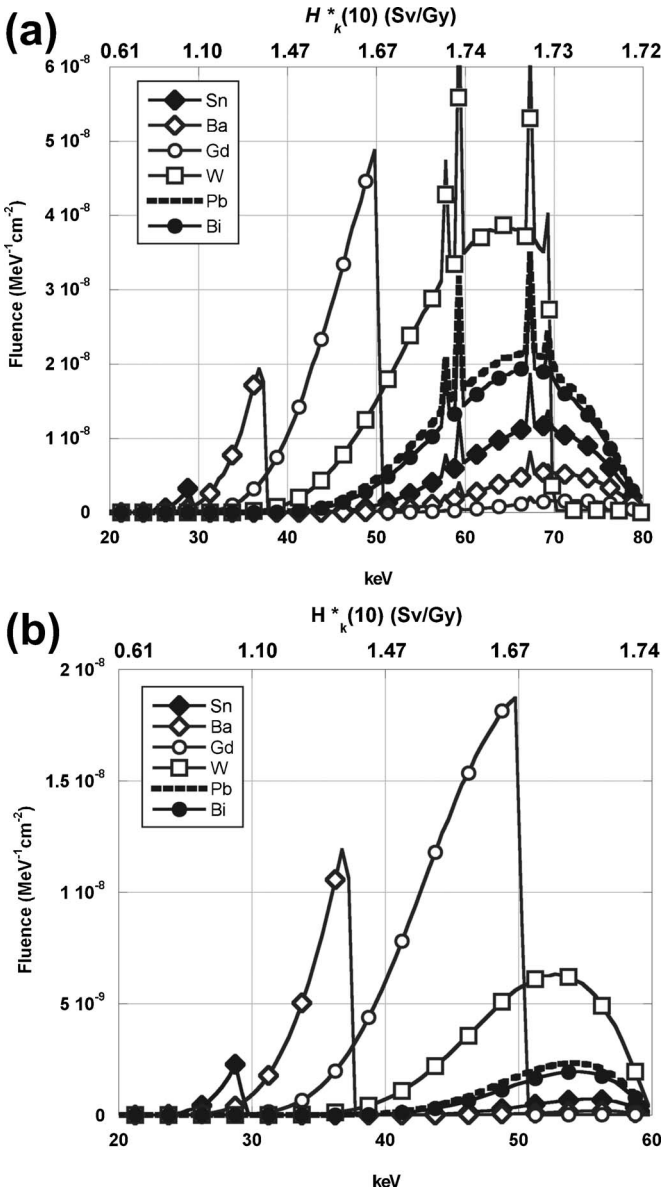

FIG. 6. Resultant spectra of (a) the 80 kVp x-ray quality and (b) the 60 kVp x-ray quality when attenuated by 0.568 g/cm^2 of six elements. Along the top x axis, the conversion coefficients $h_k^*(10)$ from air kerma, K^a to ambient dose equivalent $h^*(10)$ are given for mono-energetic photon radiation.

Some values of $H_k^*(10)$ for mono-energetic photon radiation are given at the top x-axis of Fig. 6(a) for the range from 20 to 80 keV, and Fig. 6(b) for the range from 20 to 60 keV.[13,17] Ambient dose equivalent varies significantly from air kerma over the diagnostic imaging range, and peaks at 1.74 for 60 keV mono-energetic x rays. This is primarily due to the exclusion of the backscattered component from

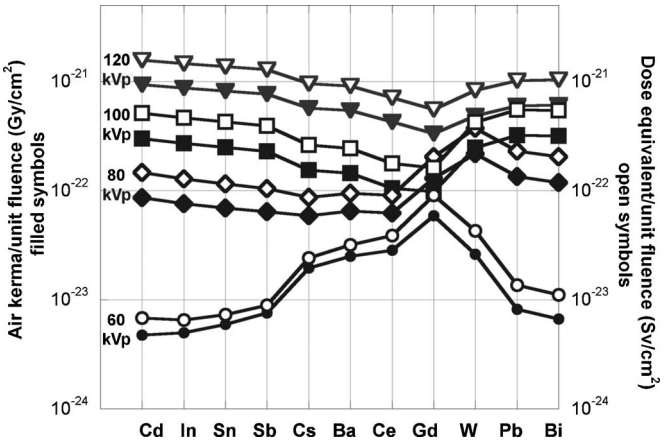

FIG. 7. EGSnrc modeling of the transmitted air kerma (filled symbols) and dose equivalent (open symbols) resulting from attenuation by 0.568 g/cm^2 of each of the elements listed along the x axis.

the measurement made free in air.[19] It is an unfortunate coincidence that the higher values of $H_k^*(10)$ are close to the energies of the tungsten $K\alpha$ emission peaks, since tungsten is the most common anode material used in x-ray tubes.

By integrating the areas under the curves in Fig. 6(a) in terms of total air kerma and total ambient dose equivalent, the spectra of the 80 kVp quality used here give an average ratio of approximately 1.6 for ambient dose equivalent (Sv) to air kerma (Gy), for all of the materials in Table I. Any shielding will lower both the total air kerma and ambient dose equivalent, but this ratio provides an interesting perspective. The spectrum produced by a thin filter of pure Pb has a ratio of 1.72 for ambient dose equivalent to air kerma due to the fact that the spectrum is peaked at higher energies. A filter of Bi with the same mass as the pure Pb also has a ratio of 1.72, but a filter of Ba, also with the same mass as Pb, has a ratio of 1.46. The lower ratio for Ba is due to increased attenuation of the more biologically damaging energies at the higher energies in the spectrum due to the position of the 37.4 keV K absorption edge. The bulk of the spectrum is contained in the peak below the absorption edge and is comprised of energies where the $H_k^*(10)$ values are lower [Fig. 6(a)]. While the integrated air kerma and ambient dose equivalent curves for both the Bi and Ba curves are less than Pb, the protection provided by the lower atomic number Ba material is superior because of increased attenuation of the higher energy radiation. This effect is in addition to the reduction in air kerma by the factor of 2.06 discussed earlier. Figure 6(b) displays the spectra of the 60 kVp quality, which lies below (at lower energies) the W $K\alpha$ peaks. The effect is that the air kerma and ambient dose equivalent ratios are lower (average of 1.40).

These variations are illustrated in Fig. 7 for the four diagnostic imaging x-ray qualities and 11 elements. The air kerma values are given by the solid symbols (left y axis) and ambient dose equivalent values are given by open symbols (right y axis). In this figure, the lower the data point (smaller y value), the lower the transmitted air kerma or ambient dose equivalent, and the more effective attenuation provided by that material at that x-ray quality. In the most extreme case (Cd), the delivered air kerma varied by a factor of 260 over these four qualities. For all four qualities, several materials provide superior attenuation compared to Pb in both air kerma and ambient dose equivalent. However, no single element provided the best protection for all qualities.

The apron materials containing lower atomic number elements (Green Lite, Sn–Ba and Hx–Pb) provided superior attenuation per unit mass than Pb-only garments at the 60, 80 and 100 kVp x-ray qualities in most cases, as reflected in the air kerma measurements shown in Figs. 4(a)–4(c) and supported by the calculations shown in Fig. 7. The 60 kV spectrum dose not include a significant contribution from the W $K\alpha$ emission lines, so the data curve for 60 kVp in Fig. 7 varies significantly in shape from those of the three higher energy x-ray qualities. The lower atomic number filters also result in lower dose equivalent values for the same reason. The peak energies in the 60 kVp spectrum correspond to the lower attenuation regions below the K absorption edges of the materials from Cs to W, resulting in large fluences which work to the disadvantage of the attenuating capabilities of these filter materials, as can be seen in Fig. 7. A similar effect is seen for W at 80 kVp.

V. CONCLUSION

Radiation shielding for diagnostic imaging energies (60–120 kVp) is mainly influenced by the position of the attenuating element's K absorption edge. The radiation shielding materials measured in this study that contained lower atomic number elements (Green Lite, Hx–Pb, Sn–Ba) provided superior attenuation per unit mass than Pb-only garments in the diagnostic imaging range in most cases. These materials also provided similar or better protection than even pure Pb per unit mass, in most cases. This is only indirectly related to the actual mass of commercial radiation shielding garments, since manufacturers must adjust the thickness of the garment and the variety of cover material to conform to a particular Pb-equivalent thickness. Attenuation provided by radiation shielding garments at the two higher energies in this study is mainly influenced by the atomic number of the attenuating metal imbedded in the polymer material, with the higher atomic numbers providing more attenuation. The W–rubber material tested here provided attenuation almost as effective in most cases as the Pb-containing materials for the two higher energy qualities as well as 100 and 120 kV in the diagnostic imaging range. Higher energy photons are only weakly attenuated by any material, so thick layers of high electron density (high Z) material are required for any significant protection.

These measurements were supported by calculations. X-ray spectra and air kerma values computed with EGSnrc user code cavity.cpp and reference spectra available through the IPEM Report 78 were in good agreement with the measured data. Modeling of the radiation attenuation capabilities of 11 elements showed a variation by a factor of about 260 for the four x-ray qualities studied here which covered the diagnostic imaging range. Calculations showed that for these

four qualities, many elements provided superior attenuation compared to Pb for both air kerma and ambient dose equivalent, but no single element provided the best protection for all qualities. This provides confidence that Monte Carlo calculations can be used to optimize the materials content of radiation shielding materials in a uniformly distributed, homogeneous material. Measurements, however, are still required to verify the actual performance of these materials.

A variety of non-Pb materials are capable of providing increased radiation protection over Pb-containing radiation shielding garments. The choice of the material is dependent on the quality of radiation requiring attenuation. A more meaningful metric of attenuation than "Pb equivalent" is needed.

ACKNOWLEDGMENTS

The authors wish to thank Carl Ross, Malcolm McEwen, and Iwan Kawrakow for helpful discussions, Infab Corporation (www.infab.org) for supplying samples of their Greenlite, HX and regular lead material, and Metal-Tech Ltd. (www.metal-tech.co.il) for the tungsten material.

[a]Electronic mail: john.mccaffrey@nrc-cnrc.gc.ca

[1]E. W. Webster, "Experiments with medium Z materials for shielding against low-energy x-rays," Radiology **86**, 146 (1966).
[2]M. J. Yaffe, G. E. Mawdsley, L. Martin, R. Servant, and R. George, "Composite materials for x-ray protection," Health Phys. **60**, 661–664 (1991).
[3]P. H. Murphy, Y. Wu, and S. A. Glaze, "Attenuation properties of lead composite aprons," Radiology **186**, 269–272 (1993).
[4]P. J. Kicken and A. J. J. Bos, "Effectiveness of lead aprons in vascular radiology: Results of clinical measurements," Radiology **197**, 473–478 (1995).
[5]E. G. Christodoulou, M. M. Soodsitt, S. C. Larson, K. L. Darner, J. Satti, and H.-P. Chan, "Evaluation of the transmitted exposure through lead equivalent aprons used in a radiology department, including contribution from backscatter," Med. Phys. **30**, 1033–1038 (2003).
[6]Y. Takano, K. Okazaki, K. Ono, and M. Kai, "Experimental and theoretical studies on radiation protective effect of a lighter non-lead protective apron," Nippon Hoshasen Gijutsu Gakkai Zasshi (Jpn. J. Radiol. Technol.) **61**, 1027–1032 (2005) (in Japanese).
[7]R. Nowotny, "XMuDat: Photon attenuation data vers. 1.0.1," Institut f. Biomed Technik u. Physik, Univ. Wien, AKH-4L, Austria, r.nowotny@bmtp.akh-wien.ac.at.
[8]IEC 1331-1, "Protective devices against diagnostic medical x-radiation," International Electrotechnical Commission, Genève, Suisse (1994).
[9]I. Kawrakow, "Accurate condensed history Monte Carlo simulation of electron transport. I. EGSnrc, the new EGS4 version," Med. Phys. **27**, 485–498 (2000).
[10]I. Kawrakow and D. W. O. Rogers, "The EGSnrc Code System: Monte Carlo simulation of electron and photon transport," Technical Report No. PIRS-701, 4th printing, National Research Council of Canada, Ottawa, Canada, 2003.
[11]I. Kawrakow, "EGSnrc C++ class library," Technical Report No. PIRS 898, National Research Council of Canada, Ottawa, Canada, 2005.
[12]E. Mainegra-Hing and I. Kawrakow, "Efficient x-ray tube simulations," Med. Phys. **33**(8), 2683–2690 (2006).
[13]K. Cranley, B. J. Gilmore, G. W. A. Fogarty, and L. Desponds, "Report No. 78: Catalogue of diagnostic x-ray spectra and other data," The Institute of Physics and Engineering in Medicine (1997).
[14]D. T. Burns, "Degrees of equivalence for the key comparison BIPM.RI(I)-K3 between national primary standards for medium energy x-rays," Summary Report for BIPM.RI(I)-K3 (2003).
[15]M. J. Berger, J. H. Hubbell, S. M. Seltzer, J. Chang, and J. S. Coursey, "XCOM: Photon Cross-Section Database," NIST, http://physics.nist.gov/PhysRefData/Xcom/Text/XCOM.html (1990).
[16]R. Birch and M. Marshall, "Computation of bremsstrahlung x-ray spectra and comparison with spectra measured with a Ge(Li) detector," Phys. Med. Biol. **24**, 505–517 (1979).
[17]International Organization for Standardization, "ISO 4037-3: X and gamma reference radiation for calibrating dosemeters and doserate meters and for determining their response as a function of photon energy–Part 3: Calibration of area and personal dosemeters and the measurement of their response as a function of energy and angle of incidence," Genève, Switzerland (1996).
[18]International Commission on Radiation Units and Measurements, ICRU Report No. 51 (1993).
[19]S. C. Klevenhagen, "Experimentally determined backscatter factors for x rays generated at voltages between 16 and 140 kV," Phys. Med. Biol. **34**, 1871–1882 (1989).